ACS APPLIED MATERIALS & INTERFACES

Research Article

www.acsami.org

Enhanced Electrical Characteristics and Stability via Simultaneous Ultraviolet and Thermal Treatment of Passivated Amorphous In–Ga–Zn–O Thin-Film Transistors

Young Jun Tak, Doo Hyun Yoon, Seokhyun Yoon, Uy Hyun Choi, Mardhiah Muhamad Sabri, Byung Du Ahn,* and Hyun Jae Kim*

School of Electrical and Electronic Engineering, Yonsei University, 50 Yonsei-ro, Seodaemun-gu, Seoul 120-749, Republic of Korea

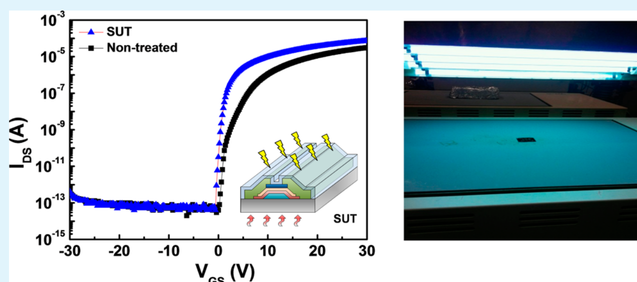

ABSTRACT: We developed a method to improve the electrical performance and stability of passivated amorphous In–Ga–Zn–O thin-film transistors by simultaneous ultraviolet and thermal (SUT) treatment. SUT treatment was carried out on fully fabricated thin-film transistors, including deposited source/drain and passivation layers. Ultraviolet (UV) irradiation disassociated weak and diatomic chemical bonds and generated defects, and simultaneous thermal annealing rearranged the defects. The SUT treatment promoted densification and condensation of the channel layer by decreasing the concentration of oxygen-vacancy-related defects and increasing the concentration of metal–oxide bonds. The SUT-treated devices exhibited improved electrical properties compared to nontreated devices: field-effect mobility increased from 5.46 to 13.36 V·s, sub-threshold swing decreased from 0.49 to 0.32 V/decade, and threshold voltage shift (for positive bias temperature stress) was reduced from 5.1 to 1.9 V.

KEYWORDS: *oxide semiconductor, thin film-transistors, In–Ga–Zn–O, UV annealing, oxygen vacancy, metal–oxide bonds*

1. INTRODUCTION

Amorphous oxide semiconductors (AOS) are promising candidates for the active layer in display backplanes because of their outstanding electrical performance compared to conventional amorphous Si thin-film transistors (TFTs).[1,2] AOS exhibit a number of advantages, including high mobility, high transparency in the visible range, low processing temperature, and excellent uniformity.[3−5] However, reliability issues, such as illumination instability, bias/current, and temperature stress plague common AOS.[6−8] These problems, which lead to deterioration in electrical performance, including negative or positive threshold voltage (V_{th}) shift, an increase or decrease in off-current, and occurrence of the hump effect, have limited the practical use of AOS, despite their advantages.[7,8]

In particular, one of the most decisive challenges to adopt AOS in display backplanes is its vulnerability to light illumination.[9] The reasons for device degradation arising from illumination are as follows: (i) photogeneration of electron–hole pairs owing to band-to-band excitation,[9,10] which is generally known as the photoconductivity in semiconductors, and (ii) phototransition of neutral oxygen vacancies to ionized oxygen vacancies.[11,12] These phenomena are intensified when the illumination wavelength is shorter, that is, under ultraviolet (UV) irradiation.

Although UV irradiation is known to degrade electrical performance, it may also enhance the electrical performance of solution-processed and vacuum-processed TFTs in the absence of a passivation layer. Kim et al. reported that appropriate UV energy readily decomposed oxygen and created ozone when oxygen was combined with disassembled monomolecular oxygen in the atmosphere.[13] Ozone, attached to the backside channel under non-passivated TFTs, induced a decrease in off-current as a result of reduced oxygen vacancies on the back surface.[13,14] In addition, Park et al. reported that UV irradiation promoted effective densification of AOS by decreasing the incidence of related impurities and promoting low processing temperatures during channel fabrication of solution-processed TFTs.[15] Thus, via photochemical activation, UV irradiation may be used to densify and condense solution-based films through cleavage of alkoxy groups.[15,16] Most efforts related to UV treatment of TFTs have focused on channel formation to lower the processing temperature in solution-processed devices and/or back-surface post-fabrication treatment of the active layer in the absence of a passivation layer to remove oxygen-vacancy-related defects.[13,14] However, UV treatment during device fabrication inevitably requires reconstruction of the overall process and equipment.

To solve this problem, we developed a method for simultaneous UV and thermal (SUT) treatment of TFTs. The method is compatible with fab-out TFTs and, thus, with conventional backplane fabrication processes. The device performance of vacuum-processed devices with a passivation

Received: December 17, 2013
Accepted: April 2, 2014
Published: April 2, 2014

 © 2014 American Chemical Society

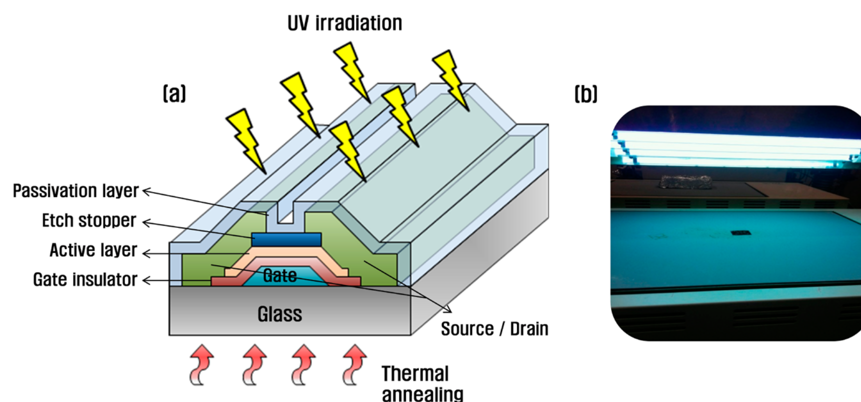

Figure 1. (a) Schematic illustration of an inverted, staggered a-IGZO TFT under SUT treatment. (b) Photograph of a device under SUT treatment.

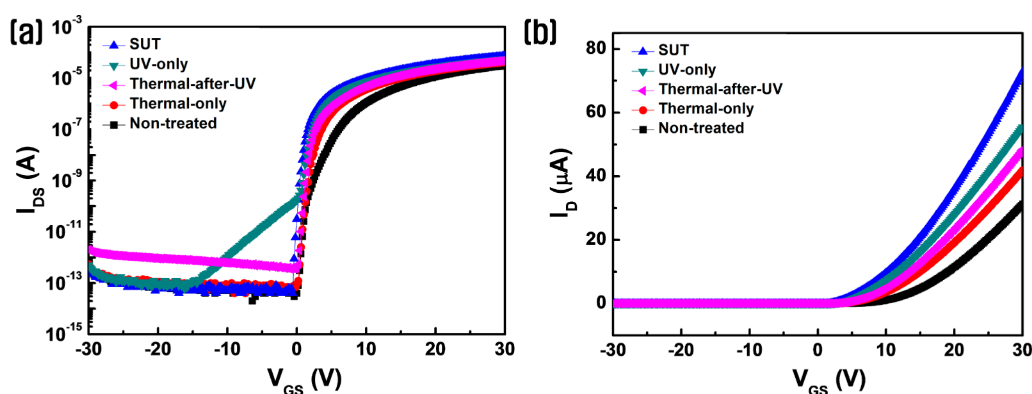

Figure 2. Transfer characteristics under different post-deposition treatments: (a) log scale and (b) linear scale.

layer has been reported to degrade under UV irradiation, based on the two mechanisms described above.[17,18] However, SUT treatment improves the electrical performance and stability of TFTs. To enhance the electrical properties of devices, various post-deposition treatments have been evaluated: high-pressure annealing,[19] plasma treatment,[20] and vacuum annealing.[21] These post-deposition treatments are costly and more complicated than SUT treatment because of the use of vacuum and pressure. SUT treatment is a low-cost, simple fabrication process that can be used to improve electrical performance with high stability. In addition, the SUT treatment step can be carried out as the last step of the fabrication process, thereby avoiding interference with existing fabrication steps. Thus, SUT post-deposition treatment can easily be implemented in industry. We evaluated the role of separate thermal annealing and UV treatments and then examined the effects of SUT treatment. To identify the role of each type of treatment, we evaluated five different sample treatments: (i) non-treated, (ii) SUT, (iii) thermal-only, (iv) UV irradiation followed by thermal (thermal-after-UV), and (v) UV-only.

2. EXPERIMENTAL SECTION

2.1. Fabrication of TFTs. The prepared TFTs had an inverted staggered structure. Using plasma-enhanced chemical vapor deposition (PECVD), a 200 nm-thick tetraethyl orthosilicate (TEOS) gate insulator was deposited at 370°C on 200 nm-thick sputtered Mo gate electrodes. The channel layer consisted of 50 nm-thick amorphous In−Ga−Zn-O (a-IGZO, target $InO_2/Ga_2O_3/ZnO$ = 2:2:1 mol %) and was deposited by sputtering and patterned via photolithography. An etch-stop layer was then deposited on 200 nm-thick SiO_2 at 300°C using PECVD, and 200 nm-thick Mo was deposited via sputtering as the photolithographically patterned source and drain electrodes. The channel length and width of the a-IGZO were 10 μm and 14 μm, respectively. Finally, PECVD was used to deposit 300 nm-thick SiO_2 as a passivation layer at 300 °C. Post-thermal annealing was performed at 300 °C in ambient air for 1 h.

2.2. Post-deposition Treatments. To investigate the individual effects of UV irradiation and thermal annealing, we performed five different post-deposition treatments on fully fabricated devices: (i) non-treated, (ii) SUT, (iii) thermal-only, (iv) thermal-after-UV, and (v) UV-only. The fabricated devices were irradiated using a light-emitting diode based UV lamp with a wavelength of 365 nm and a photon flux density of 254 mW/cm^2. Then, thermal annealing was carried out at 200°C in ambient air on a hot plate. Both UV irradiation and thermal annealing were performed for 30 min. Figure 1a shows a schematic diagram of the device structure under SUT treatment, and Figure 1b presents a photograph of the experimental SUT treatment, in which UV irradiation and thermal annealing were simultaneously performed.

2.3. Electrical and Chemical Measurements. We measured the electrical characteristics of the devices subjected to different post-deposition treatments using an HP4156C semiconductor parameter analyzer in the dark at room temperature. To evaluate the stability of different post-deposition treated devices, a positive bias temperature stress (PBTS) was applied (V_{GS} = 20 V and V_{DS} = 0.1 V at 60 °C for 15 000 s), and treated devices were re-measured after 7 days to evaluate the persistence of the effect of the post-deposition treatments. To further evaluate the SUT treatment, we also performed X-ray photoelectron spectroscopy (XPS) to analyze the quantitative and qualitative changes in surface composition and chemical structure. Spectroscopic ellipsometry was performed in conjunction with XPS to measure the optical band gap and to facilitate band alignment with respect to the band gap and valence band offset.

3. RESULTS AND DISCUSSION

3.1. Electrical Characteristics of Post-deposition Treated a-IGZO TFTs. Figure 2a shows the log scale transfer characteristics of the drain current under different post-deposition treatments, and Figure 2b shows the linear transfer characteristics of the drain current. As indicated in Figure 2, SUT-treated devices exhibited superior electrical performance compared with other treated devices. However, UV-only and thermal-after-UV treated devices exhibited the hump effect and an increase in off current. These buildups were attributed to the creation of additional current paths in the channel layer and an increase in carrier concentration, respectively.[22] In the UV-only treated samples, UV irradiation induced a broad distribution of oxygen vacancies that photo-transitioned to ionized oxygen vacancies near the conduction band minimum on shallow donor states, photo-generated electron−hole pairs in the sub-gap region, and photodecomposition of weak chemical bonds.[10−12,23] Among these effects, photo-transitioning was most related to the induced hump effect when gate bias was applied.[23]

In the thermal-after-UV treated samples, decomposed chemical bonds and ionized oxygen vacancies generated by UV irradiation were unstable and unlikely to rearrange because the time interval prior to thermal annealing. In other words, non-reorganized atoms, which consisted of interstitial atoms and oxygen species in the sub-gap, acted as charge carriers and defect sites.[22,24] For these reasons, electrical performance deteriorated under UV-only and thermal-after-UV treatments. In contrast, thermal-only treated samples exhibited a small improvement in electrical performance, because thermal annealing partially induced rearrangement of existing weak chemical bonds and interstitial atoms in pristine devices. In SUT-treated samples, decomposition and rearrangement occurred simultaneously; therefore, SUT-treated devices exhibited superior electrical performance compared with other post-deposition treated devices.

Table 1 summarizes the electrical parameters for different post-deposition treatments, including field-effect mobility (μ_{FET}), on/off ratio, subthreshold swing (SS), and maximum trapped charge density (N_{max}). The μ_{FET} was determined by maximum trans-conductance at a drain voltage of 10.1 V. The SS value corresponded to the amount of gate voltage change required to increase I_{DS} by one order of magnitude in the sub-threshold region. N_{max} was extracted from the transfer characteristics using the relationship

Table 1. Summary of the Device Electrical Parameters, Including μ_{FET}, On/Off Ratio, SS, and N_{max} for Different Post-deposition Treatments

sample	μ_{FET} (cm^2/V·s)	on/off ratio	SS (V/decade)	N_{max} (cm^{-2})
non-treated	5.49	1.57×10^9	0.49	7.13×10^{11}
thermal-only	6.10	1.05×10^9	0.41	5.80×10^{11}
SUT	13.36	1.82×10^9	0.32	4.31×10^{11}
UV-only	10.21	9.24×10^8	0.76	1.16×10^{12}
thermal-after-UV	7.06	1.38×10^8	0.41	5.80×10^{11}

$$N_{max} = \left(\frac{SS \bullet \log(e)}{kT/q} - 1\right)\frac{C_i}{q}$$

where k is the Boltzmann constant, T is the absolute temperature, C_i is the gate capacitance per unit area, and q is the elementary charge.

3.2. Stability of Post-deposition-Treated a-IGZO TFTs. Stability is also critical to prolonging device operation in displays. To compare V_{th} shift variation under PBTS, different post-deposition treated devices were measured at V_{GS} = 20 V and V_{DS} = 0.1 V at 60 °C for 15 000 s. Positive V_{th} shift originates from negative charges in the channel region trapped at the channel/gate insulator interface during stability testing.[25,26] Figure 3 shows V_{th} shift under PBTS for different post-deposition treatments as a function of stress time. While the V_{th} shift of non-treated devices was 5.1 V, the V_{th} shift of SUT-treated devices was 1.9 V. The V_{th} shifts of thermal-only, thermal-after-UV, and UV-only treatment were 4.8, 5.4, and 6.5 V, respectively. Thus, SUT treatment effectively decreases the trapped concentration of negative charges and defect sites caused by interstitial atoms and oxygen vacancies.

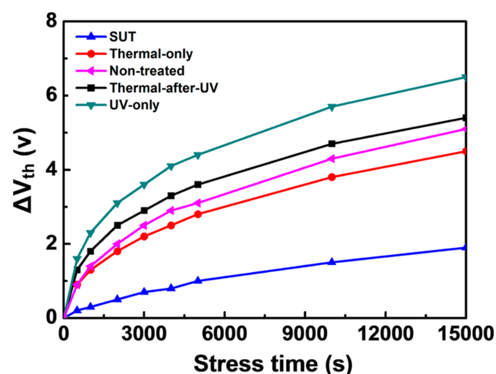

Figure 3. Variation of PBTS-induced V_{th} shift for different post-deposition treated devices as a function of the stress time.

We also remeasured the performance of UV-only and SUT-treated devices after 7 days to determine whether these post-deposition treatment effects were temporary. Previous reports suggested that electrical characteristics are altered under UV irradiation by photo-generated carrier recombination and ionized oxygen vacancy neutralization.[11,12] As shown in Figure 4, the transfer characteristics of UV-only treated devices gradually shifted upon device aging, while the enhanced transfer characteristics of SUT-treated devices were maintained, even after 7 days. Therefore, SUT-treated devices were not affected by photogenerated carrier recombination or ionized oxygen vacancy neutralization.

3.3. a-IGZO Chemical Bond Disruptions by SUT Treatment. Although the mechanisms of UV treatment on solution-processed TFTs[15,16] and ozone treatment[13,14] have been extensively studied, the SUT treatment mechanism has not been reported. We proposed a simple mechanism, illustrated in Figure 5. Hosono et al. reported that the bond energy of diatomic formations for In−O, Ga−O, and Zn−O in a-IGZO TFTs are ∼1.7, ∼2.0, and ∼1.5 eV, respectively, calculated using density functional theory.[27] The bond energy, which is determined by chemical bond strength, is defined as the minimum energy required to dissociate a diatomic species into individual atoms.[28] Therefore, a chemical bond can be broken when the applied external energy exceeds the bond energy.[27,28] For example, the diatomic In−O, Ga−O, and Zn−O bonds in the a-IGZO sub-gap region can be broken by UV

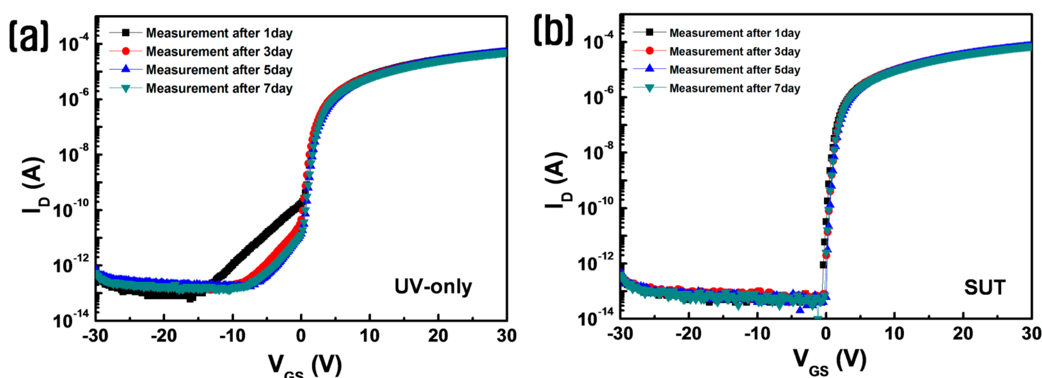

Figure 4. Transfer characteristics after post-deposition treatments after 1, 3, 5, and 7 days for (a) a UV-only treated device and (b) an SUT-treated device.

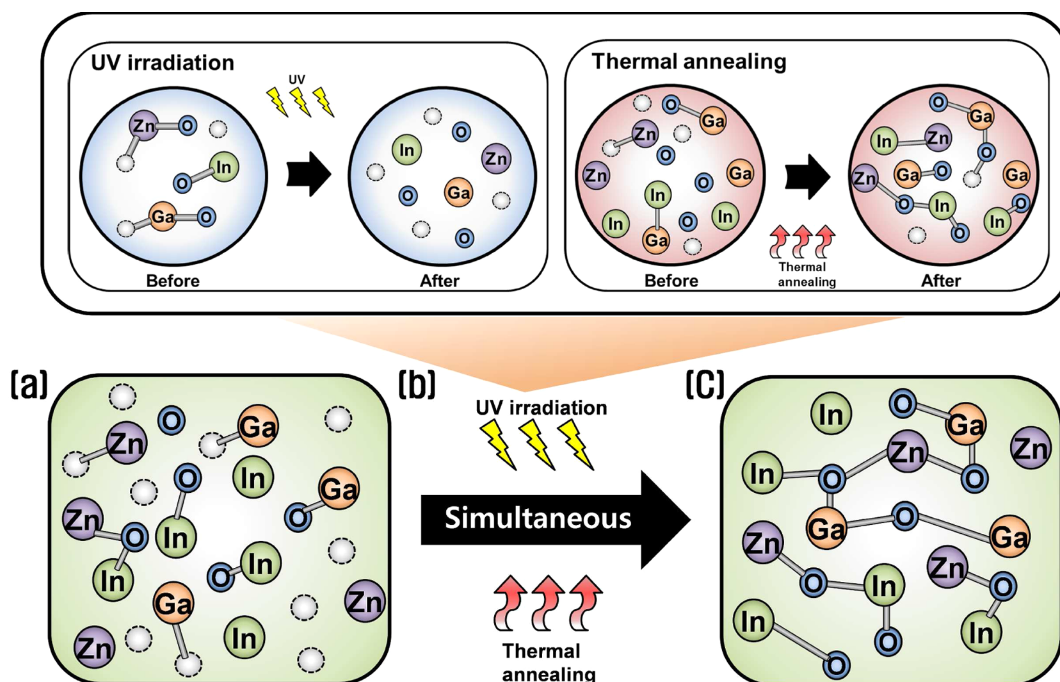

Figure 5. Proposed, simple SUT treatment: (a) Prior to SUT treatment, (b) under SUT treatment, and (c) after SUT treatment.

irradiation of higher energy than the bond energy. The UV irradiation energy was determined by the Planck relationship:

$$E = \frac{hc}{\lambda}$$

where h, c, and λ are the Planck constant, the light velocity, and the light wavelength, respectively. From this relationship, at a wavelength of 365 nm, an energy of 3.4 eV was calculated, which is higher than the In−O, Ga−O, and Zn−O diatomic bond formation energies. At this wavelength, the energy was sufficient to decompose weak and diatomic chemical bonds and to increase the concentration of defect sites. However, the thermal energy supplied by 200°C, which is ~0.04 eV, was not sufficient to dissociate the chemical bonds. However, it was just enough to induce atomic rearrangement and reorganization, due to the activation energy of decomposed atoms and defect sites, eventually resulting in chemical bond formation and a reduction in the concentration of defect sites.[23,29−32] As shown in Figure 5a, because of the intrinsic properties of AOS, weak and diatomic chemical bonds, interstitial atoms, and defect-related oxygen vacancies existed in non-treated devices. However, under SUT treatment, UV irradiation induced the decomposition of weak and diatomic chemical bonds, photo-transition of oxygen vacancies, and photo-generation of electron−hole pairs.[12,23] As a result, dissociated atoms and defect sites were more abundant in SUT-treated devices than in non-treated devices. Upon decomposition, thermal annealing contributed to the reorganization of dissociated atoms and reduced the concentration of defects related to interstitial atoms and oxygen vacancies,[29,30] as illustrated in Figure 5b. The simultaneous decomposition and rearrangement is the essence of SUT treatment and critical to enhancing device performance. Therefore, SUT treatment improved the quality of the channel layer because of a reduction in the concentration of defect-related oxygen vacancies and an increase in the chemical bonds, as illustrated in Figure 5c.

3.4. XPS Analysis of Post-deposition-Treated a-IGZO TFTs. We performed XPS analysis to examine the influence of SUT treatment on the surface composition and chemical structural changes related to oxygen. Figure 6 presents the O 1s spectra for an a-IGZO film with different post-deposition treatments. The spectra were deconvoluted as Gaussian

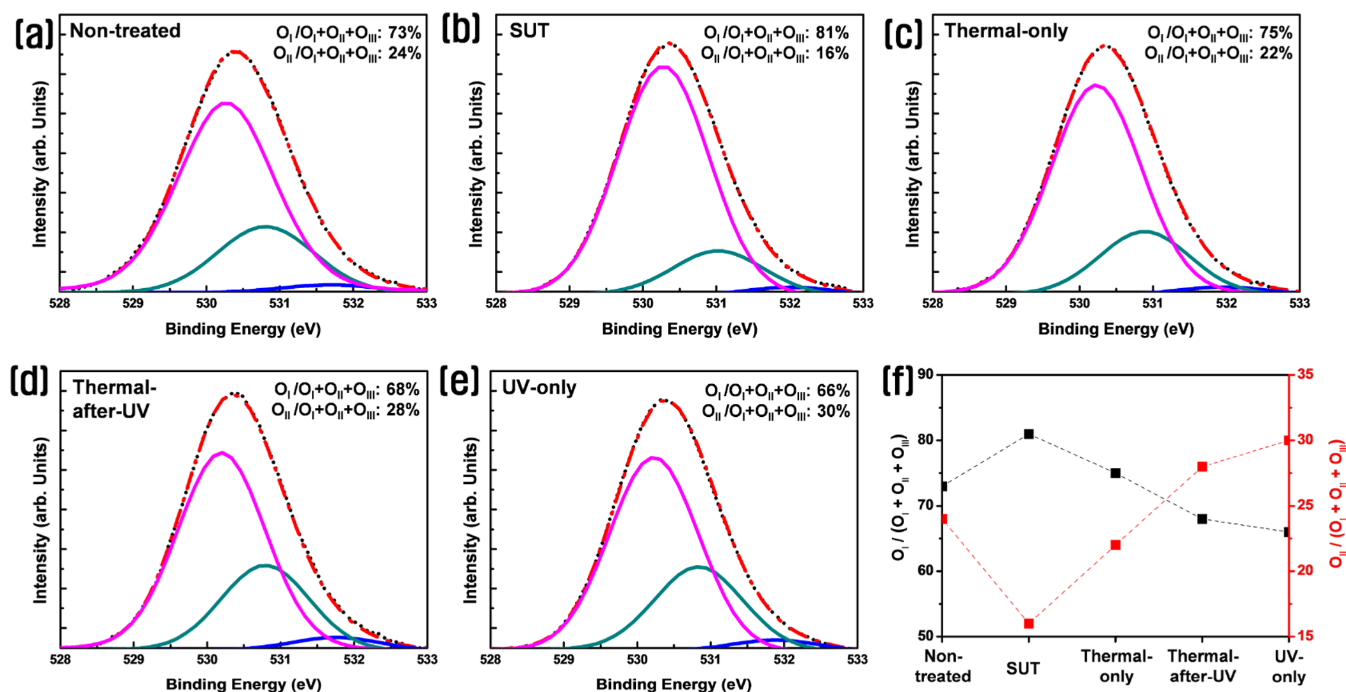

Figure 6. XPS results for the O 1s peak for an a-IGZO film under different post-deposition treatments: (a) non-treated, (b) SUT, (c) thermal-only, (d) thermal-after-UV, and (e) UV-only. (f) Comparison of the area for both low binding energy and middle binding energy as a function of the post-deposition treatment.

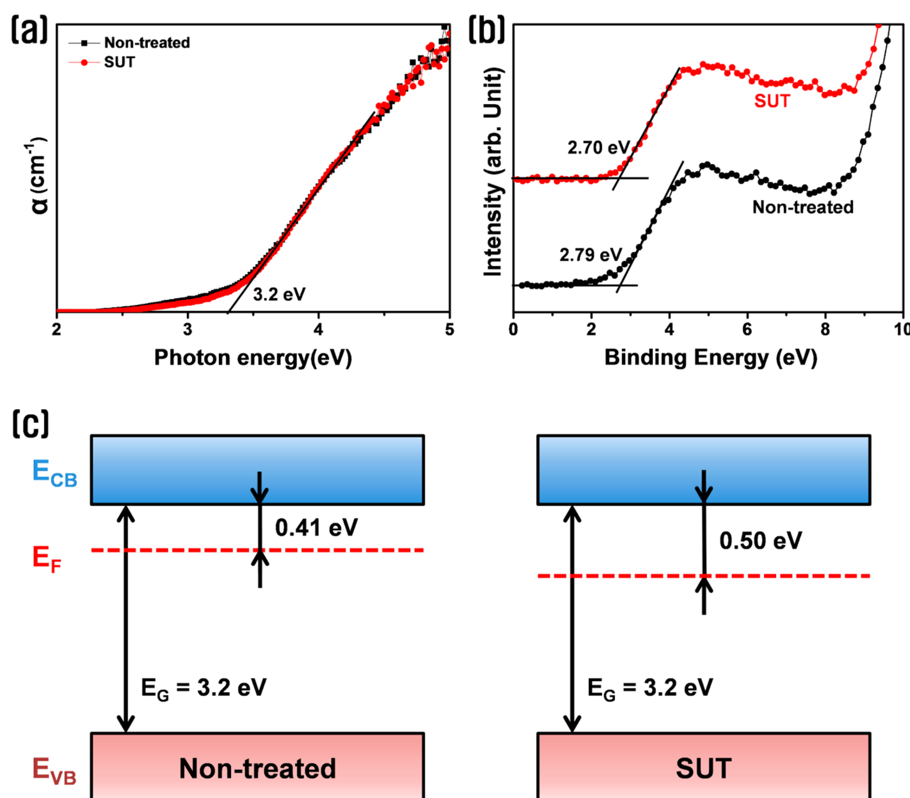

Figure 7. (a) Absorption coefficient spectra of the non-treated and SUT-treated devices using spectroscopic ellipsometry. (b) Valence band offset spectra of non-treated and SUT-treated devices using XPS. (c) Band alignment in non-treated and SUT-treated devices.

distributions after correcting for the background. The O 1s spectra were consistently divided into three different peaks located at 530.1 ± 0.1, 531.0 ± 0.2, and 532.0 ± 0.1. The first peak is characteristic of a material with a low binding energy (O_I), originating from lattice oxygen related to Zn, In, and Ga metal−oxide (M−O) bonds. The middle binding energy (O_{II}) and high binding energy (O_{III}) peaks correspond to non-lattice oxygen atoms, such as those in oxygen-deficient (V_o) regions

and loosely bonded hydroxyl groups, respectively.[33,34] The SUT-treated devices exhibited an 8% increase in area related to M-O bonds and a 6% decrease in area related to V_o compared with non-treated devices. On the basis of our explanation above, SUT treatment effectively reduced the concentration of defects related to V_o and promoted atomic rearrangement in a-IGZO films. In UV-only treated devices, the area associated with M−O bonds was the lowest and V_o was the highest because no driving force for reorganizing dissociated chemical bonds, interstitial atoms, and defect sites existed. Thermal-after-UV treated devices exhibited fewer M−O bonds and higher V_o compared with non-treated devices; this result was attributed to unstable decomposition of chemical bonds and ionized V_o arising from UV irradiation, which inhibited rearrangement because of the time interval between UV and thermal treatments. However, devices treated with thermal-only exhibited slightly higher M−O bonds and lower V_o than non-treated devices, which were attributed to rearrangement of existing weak chemical bonds, interstitial atoms, and defects originating from the intrinsic amorphous properties of the material.

In summary, the role of UV irradiation is to decrease the concentration of M-O and increase V_o, and the role of thermal annealing is atomic rearrangement[31,32] and removal of defect sites in the channel layer.[25]

3.5. Band Alignment of SUT-Treated a-IGZO TFTs.

Figure 7a and b shows the optical band-gap and valence band spectra of non-treated and SUT-treated devices, respectively. The optical band gap of the SUT-treated device was nearly the same as that of non-treated devices, suggesting that the overall atomic composition of the channel layer was not influenced by SUT treatment.[35] The valence band offset decreased from 2.79 to 2.70 eV after SUT treatment, as shown in Figure 7b. This decrease in valence band offset resulted in an increase in the conduction band offset from 0.41 to 0.50 eV, as shown in Figure 7c. The change in conduction band offset suggested a decrease in carrier concentration arising from a reduction in V_o[29] and interstitial atoms,[36,37] which is consistent with XPS results. In other words, defects related to V_o[38,39] and interstitial atoms in the channel layer were reduced, resulting in enhanced electrical performance and device stability.[38−40] Therefore, SUT-treated devices exhibited superior electrical properties and stability because of an increase in the concentration of M−O bonds and a decrease in defects.

4. CONCLUSION

We performed post-deposition SUT treatment on passivated a-IGZO TFTs to improve the electrical performance and stability of devices. The μ_{FET} increased from 5.49 (non-treated) to 13.36 $cm^2/V \cdot s$ after SUT treatment. SUT treatment results in the highest μ_{FET} among the post-deposition treatments evaluated. PBTS and re-measurement after 7 days were carried out to investigate stability and durability of the device, respectively. SUT-treated devices exhibited a small V_{th} shift of 1.9 V under 15 000 s of bias stress and retained the enhanced transfer characteristics after 7 days. SUT treatment effectively induced the accelerated formation of M−O bonds, atomic modification, and a reduction in defects. In our proposed SUT treatment, UV irradiation caused dissociation of chemical bonds and increased the concentration of oxygen vacancies. Simultaneous atomic rearrangement and modification were induced by thermal annealing. We concluded that UV irradiation and thermal annealing should be performed simultaneously to provide effective decomposition and rearrangement in a-IGZO TFTs. In summary, SUT treatment, which consists of a simple and permanent post-deposition treatment without the use of vacuum or pressure, improved the electrical properties and stability of devices.

AUTHOR INFORMATION

Corresponding Authors

*E-mail: bdahn@yonsei.ac.kr.

*E-mail: hjk3@yonsei.ac.kr.

Notes

The authors declare no competing financial interest.

ACKNOWLEDGMENTS

This work was supported by the National Research Foundation of Korea (NRF) grant funded by the Korean Ministry of Education, Science and Technology (MEST) [no. 2011-0028819].

REFERENCES

(1) Nomura, K.; Ohta, H.; Takagi, A.; Kamiya, T.; Hirano, M.; Hosono, H. Room-Temperature Fabrication of Transparent Flexible Thin-Film Transistors Using Amorphous Oxide Semiconductors. *Nature* **2004**, *432*, 488−491.

(2) Hosono, H. Ionic Amorphous Oxide Semiconductors: Material Design, Carrier Transport, and Device Application. *J. Non-Cryst. Solids* **2006**, *352*, 851−858.

(3) Fortunate, E.; Barquinha, P.; Pimentel, A.; Goncalves, A.; Marques, A. Wide-Bandgap High-Mobility ZnO Thin-Film Transistors Produced at Room Temperature. *Appl. Phys. Lett.* **2004**, *85*, 2541.

(4) Chiang, H.; Wager, J.; Hoffman, R.; Jeong, J.; Keszler, D. High Mobility Transparent Thin-Film Transistors with Amorphous Zinc Tin Oxide Channel Layer. *Appl. Phys. Lett.* **2005**, *86*, No. 013503.

(5) Nomura, K.; Ohta, H.; Ueda, K.; Kamiya, T.; Hirano, M.; Hosono, H. Thin-Film Transistor Fabricated in Single-Crystalline Transparent Oxide Semiconductor. *Science* **2003**, *300*, 1269−1272.

(6) Suresh, A.; Muth, J. Bias Stress Stability of Indium Gallium Zinc Oxide Channel Based Transparent Thin Film Transistors. *Appl. Phys. Lett.* **2008**, *92*, No. 033502.

(7) Su, B.-Y.; Chu, S.-Y.; Juang, Y.-D.; Liu, S.-Y. Effects of Mg Doping on the Gate Bias and Thermal Stability of Solution-Processed InGaZnO Thin-Film Transistors. *J. Alloys Compd.* **2013**, *580*, 10−14.

(8) Ryu, B.; Noh, H.-K.; Choi, E.-A.; Chang, K. J. O-Vacancy as the Origin of Negative Bias Illumination Stress Instability in Amorphous In−Ga−Zn−O Thin Film Transistors. *Appl. Phys. Lett.* **2010**, *97*, No. 022108.

(9) Barquinha, P.; Pimentel, A.; Marques, A.; Pereira, L.; Martins, R.; Fortunato, E. Effect of UV and Visible Light Radiation on the Electrical Performances of Transparent TFTs Based on Amorphous Indium Zinc Oxide. *J. Non-Cryst. Solids* **2006**, *352*, 1756−1760.

(10) Seo, S.-J.; Jeon, J. H.; Hwang, Y. H.; Bae, B.-S. Improved Negative Bias Illumination Instability of Sol-Gel Gallium Zinc Tin Oxide Thin Film Transistors. *Appl. Phys. Lett.* **2011**, *99*, No. 152102.

(11) Yu, K. M.; Jeong, S. H.; Bae, B. S.; Yun, E. J. The Effect of UV Treatment on the Recovery Characteristics of a-IGZO-based Thin Film Transistors. *J. Korean Phys. Soc.* **2012**, *61*, 852−857.

(12) Takechi, K.; Nakata, M.; Eguchi, T.; Yamaguchi, H.; Kaneko, S. Comparison of Ultraviolet Photo-Field Effects between Hydrogenated Amorphous Silicon and Amorphous $InGaZnO_4$ Thin-Film Transistors. *Jpn. J. Appl. Phys.* **2009**, *48*, No. 010203.

(13) Chong, H. Y.; Lee, S. H.; Kim, T. W. Effect of an Ultraviolet-Ozone Treatment on the Electrical Properties of Titanium-Oxide Thin-Film Transistors Fabricated by Using Sol−Gel Process. *J. Electrochem. Soc.* **2012**, *159*, B771−B774.

(14) Liu, P.; Chen, T. P.; Li, X. D.; Liu, Z.; Wong, J. I.; Liu, T.; Leong, K. C. Effect of Exposure to Ultraviolet-Activated Oxygen on the Electrical Characteristics of Amorphous Indium Gallium Zinc

Oxide Thin Film Transistors. *Electrochem. Solid State Lett.* **2013**, *2*, Q21−Q24.

(15) Kim, Y.-H.; Heo, J.-S.; Kim, T.-H.; Park, S.; Yoon, M.-H.; Kim, J.; Oh, M. S.; Yi, G.-R.; Noh, Y.-Y.; Park, S. K. Flexible Metal-Oxide Devices made by Room Temperature Photochemical Activation of Sol−Gel Films. *Nature* **2012**, *489*, 128−132.

(16) Lee, J. S.; Song, S. M.; Kang, D. W.; Kim, Y. H.; Kwon, J. Y.; Han, M. K. Effects of Ultra-Violet Treatment on Electrical Characteristics of Solution-processed Oxide Thin-Film Transistors. *ECS Trans.* **2012**, *50*, 121−127.

(17) Um, J. G.; Mativenga, M.; Migliorato, P.; Jang, J. Increase of Interface and Bulk Density of States in Amorphous−Indium−Gallium−Zinc Oxide Thin-Film Transistors with Negative-Bias-Under-Illumination-Stress Time. *Appl. Phys. Lett.* **2012**, *101*, No. 113504.

(18) Lee, S.-Y.; Kwon, J.-Y.; Han, M.-K. Investigation of Photo-Induced Hysteresis and Off-Current in Amorphous In−Ga−Zn Oxide Thin-Film Transistors Under UV Light Irradiation. *IEEE Trans. Electron Devices* **2013**, *60*, 2574−2579.

(19) Ji, K. H.; Kim, J. I.; Jung, H. Y.; Park, S. Y.; Choi, R. Effect of High-Pressure Oxygen Annealing on Negative Bias Illumination Stress-Induced Instability of InGaZnO Thin Film Transistors. *Appl. Phys. Lett.* **2011**, *98*, No. 103509.

(20) Park, J. S.; Jeong, J. K.; Mo, Y.-G.; Kim, H. D.; Kim, S.-I. Improvements in the Device Characteristics of Amorphous Indium Gallium Zinc Oxide Thin-Film Transistors by Ar Plasma Treatment. *Appl. Phys. Lett.* **2007**, *90*, No. 262106.

(21) Yuan, Z.; Zhu, X.; Wang, X.; Cai, X.; Zhang, B.; Qiu, D.; Wu, H. Annealing Effects of In_2O_3 Thin Films on Electrical Properties and Application in Thin Film Transistors. *Thin Solid Films* **2011**, *519*, 3254−3258.

(22) Kim, Y.-M.; Jeong, K.-S.; Yun, H.-J.; Yang, S.-D.; Lee, S.-Y. Investigation of Zinc Interstitial Ions as the Origin of Anomalous Stress Induced Hump in Amorphous Indium Gallium Zinc Oxide Thin Film Transistors. *Appl. Phys. Lett.* **2013**, *102*, No. 173502.

(23) Rim, Y. S.; Jeong, W.; Ahn, B. D.; Kim, H. J. Defect Reduction in Photon-Accelerated Negative Bias Instability of InGaZnO Thin-Film Transistors by High-Pressure Water Vapor Annealing. *Appl. Phys. Lett.* **2013**, *102*, No. 143503.

(24) Chang, H.-J.; Huang, K.-M.; Chen, S.-F.; Huang, T.-H.; Wu, M.-C. RF Sputtered Low-Resistivity and High-Transmittance Indium Gallium Zinc Oxide Films for Near-UV Applications. *Electrochem. Solid State Lett.* **2011**, *14*, H132−H134.

(25) Nomura, K.; Kamiya, T.; Kikuchi, Y.; Hirano, M.; Hosono, H. Comprehensive Studies on the Stabilities of a-In−Ga−Zn−O Based Thin Film Transistor by Constant Current Stress. *Thin Solid Films* **2010**, *518*, 3012−3016.

(26) Kim, C. H.; Rim, Y. S.; Kim, H. J. Chemical Stability and Electrical Performance of Dual-Active-Layered Zinc−Tin−Oxide/Indium−Gallium−Zinc−Oxide Thin-Film Transistors Using a Solution Process. *ACS Appl. Mater. Interfaces* **2013**, *5*, 6108−6112.

(27) Kamiya, T.; Nomura, K.; Hosono, H. Subgap States, Doping and Defect Formation Energies in Amorphous Oxide Semiconductor a-$InGaZnO_4$ Studied by Density Functional Theory. *Phys. Status Solidi A* **2010**, *207*, 1698−1703.

(28) Aikawa, S.; Nabatame, T.; Tsukagoshi, K. Effects of Dopants in InOx-Based Amorphous Oxide Semiconductors for Thin-Film Transistor Applications. *Appl. Phys. Lett.* **2013**, *103*, No. 172105.

(29) Ahn, B. D.; Lim, J. H.; Cho, M.-H.; Park, J.-S.; Chung, K.-B. Thin-Film Transistor Behavior and the Associated Physical Origin of Water-Annealed In−Ga−Zn Oxide Semiconductor. *J. Phys. D: Appl. Phys.* **2012**, *45*, No. 415307.

(30) Takechi, K.; Nakata, M.; Eguchi, T.; Yamaguchi, H.; Kaneko, S. Temperature-Dependent Transfer Characteristics of Amorphous InGaZnO4 Thin-Film Transistors. *Jpn. J. Appl. Phys.* **2009**, *48*, No. 011301.

(31) Chiang, H. Q.; Wager, J. F.; Hoffman, R. L.; Jeong, J.; Keszler, D. A. High Mobility Transparent Thin-Film Transistors with Amorphous Zinc Tin Oxide Channel Layer. *Appl. Phys. Lett.* **2005**, *86*, No. 013503.

(32) Fortunato, E.; Pereira, L.; Barquinha, P.; Bothelho do Rego, A.; Goncalves, G. High Mobility Indium Free Amorphous Oxide Thin Film Transistors. *Appl. Phys. Lett.* **2008**, *92*, No. 222103.

(33) Kang, J. H.; Cho, E. N.; Kim, C. E.; Lee, M. J.; Lee, S. J. Mobility Enhancement in Amorphous InGaZnO Thin-Film Transistors by Ar Plasma Treatment. *Appl. Phys. Lett.* **2013**, *102*, No. 222103.

(34) Chen, M.; Pei, Z. L.; Sun, C.; Wen, L. S.; Wang, X. Surface Characterization of Transparent Conductive Oxide Al-doped ZnO Films. *J. Cryst. Growth* **2000**, *220*, 254−262.

(35) Ahn, C. H.; Kim, J. H.; Cho, H. K. Tunable Electrical and Optical Properties in Composition Controlled Hf:ZnO Thin Films Grown by Atomic Layer Deposition. *J. Electrochem. Soc.* **2012**, *159*, H384−H387.

(36) Kwon, S.; Bang, S.; Lee, S.; Jeon, S.; Jeong, W.; Kim, H.; Gong, S. C.; Chang, H. J.; Park, H.-H.; Jeon, H. Characteristics of the ZnO Thin Film Transistor by Atomic Layer Deposition at Various Temperatures. *Semicond. Sci. Technol.* **2009**, *24*, No. 035015.

(37) Alford, T. L.; Gadre, M. J.; Vemuri, N. P. Improved Mobility and Transmittance of Room-Temperature-Deposited Amorphous Indium Gallium Zinc Oxide (a-IGZO) Films with Low-Temperature Post fabrication Anneals. *JOM* **2013**, *65*, 519−524.

(38) Noh, H.-K.; Chang, K. J.; Ryu, B.; Lee, W. J. Electronic Structure of Oxygen-Vacancy Defects in Amorphous In-Ga-Zn-O Semiconductors. *Phys. Rev. B* **2011**, *84*, No. 115205.

(39) Zan, H.-W.; Yeh, C.-C.; Meng, H.-F.; Tsai, C.-C.; Chen, L.-H. Achieving High Field-Effect Mobility in Amorphous Indium- Gallium-Zinc Oxide by Capping a Strong Reduction Layer. *Adv. Mater.* **2012**, *24*, 3509−3514.

(40) Murat, A.; Adler, A. U.; Mason, T. O.; Medvedeva, J. E. Carrier Generation in Multicomponent Wide-Bandgap Oxides: $InGaZnO_4$. *J. Am. Chem. Soc.* **2013**, *135*, 5685−5692.